chemosensors

MDPI

Article

Fabrication of Functional Super-Hydrophilic TiO_2 Thin Film for pH Detection

Cheng Chen [1], Yalei Zhang [1], Han Gao [1], Kun Xu [1,2] and Xiliang Zhang [1,*]

[1] School of Mechanical Engineering, Jiangsu University, Zhenjiang 212013, China; 2111603001@stmail.ujs.edu.cn (C.C.); 2212003095@stmail.ujs.edu.cn (Y.Z.); 2232003002@stmail.ujs.edu.cn (H.G.); k.xu018@haut.edu.cn (K.X.)
[2] College of Electrical Engineering, Henan University of Technology, Zhengzhou 450001, China
* Correspondence: zhangxl@ujs.edu.cn

Abstract: A super-hydrophilic pH-sensitive electrode with a porous TiO_2 thin film is proposed in this work and fabricated using the chemical etching method. In total, 30 groups of porous TiO_2 thin film were obtained by immersing a Ti sheet in NaOH, with the solution concentration ranging from 0.5–4 M and the reaction time ranging from 15–240 min. SEM, XRD, XPS, and a contact angle meter were used to investigate the influence of the chemical etching parameters on the morphology, composition, and wettability of the fabricated electrodes. The chemical etching parameters were found to have a significant influence on the specific surface area and the component of the films, which strongly affected the wettability and pH sensing characteristics of the electrodes. The electrode obtained with a solution concentration of 1 M and reaction time of 120 min is the ideal product because of its excellent wettability, with a contact angle of 5.46°, and good pH sensing characteristics in pH buffer solutions. The electrode also showed good stability regarding its wettability and pH sensing properties during storage and utilization.

Keywords: pH-sensitive electrode; super-hydrophilic; TiO_2 thin film; chemical etching

check for updates

Citation: Chen, C.; Zhang, Y.; Gao, H.; Xu, K.; Zhang, X. Fabrication of Functional Super-Hydrophilic TiO_2 Thin Film for pH Detection. *Chemosensors* **2022**, *10*, 182. https://doi.org/10.3390/chemosensors10050182

Received: 14 April 2022
Accepted: 7 May 2022
Published: 11 May 2022

Publisher's Note: MDPI stays neutral with regard to jurisdictional claims in published maps and institutional affiliations.

Copyright: © 2022 by the authors. Licensee MDPI, Basel, Switzerland. This article is an open access article distributed under the terms and conditions of the Creative Commons Attribution (CC BY) license (https://creativecommons.org/licenses/by/4.0/).

1. Introduction

In 1997, Fujishima demonstrated the super-hydrophilic effect of a TiO_2 polycrystalline film exposed to UV [1]. Since then, super-hydrophilic surfaces have been extensively applied, such as for improving the performance of sensors. Humidity sensors based on super-hydrophilic surfaces were found to show the advantages of a high sensitivity, fast response, and short recovery time [2,3]. A super-hydrophilic surface has an extremely low contact angle and allows fast spreading of water on its surface. Thus, a small water drop can cover a large area of the super-hydrophilic surface, producing a large effective area for electrochemical reaction and thus improving the pH sensing performance [4–6].

pH sensors based on metal oxides, such as RuO_2, ZnO, SnO_2, TiO_2, and V_2O_5, are alternatives to glass electrodes and have the advantages of good stability over a wide pH range, high mechanical robustness, miniaturization, wide-ranging working temperature, and a fast response in aqueous or non-aqueous environments [7]. Among pH sensing metal oxides, TiO_2 is a promising material for new pH sensors owing to its superior chemical stability, non-toxicity, relatively inexpensive costs, and easy fabrication. Various methods have been proposed for TiO_2 films for pH detection. Yao reported a sol-gel TiO_2 pH sensor that was deposited on ITO glass and post-annealed at 200 °C, which showed a sensitive response of 79.9 μA/pH [8]. Yusof used an RF magnetron sputtering system to fabricate a TiO_2 sensing membrane of an EGFET pH sensor, which showed a Nernstian response of 59.89 mV/pH [9]. Huang prepared a pH sensor with TiO_2 nanowire arrays using the hydrothermal growth method, and a sensitivity of 62 mV/pH was detected [10]. Doghmane used the spin coating method to fabricate a TiO_2- and AgCl-based pH sensor with a sensitivity of 45.229 mV/pH [11].

TiO_2 has also received significant attention regarding its application on super-hydrophilic surfaces. Anatase-phase TiO_2 has a good hydrophilic ability and can become a super-hydrophilic surface when exposed to UV [1,12]. Zhao reported that the sensitivity of a pH sensor based on TiO_2 nanotube arrays increased from 54.5 to 59 mV/pH and achieved good hydrophilicity when UV mediation was used [5]. However, the hydrophilic TiO_2 films obtained using UV mediation reportedly became hydrophobic within several hours or several days of storage [13–15].

The fabrication of a microstructure with a large specific surface area on its surface is another method that is used to obtain a super-hydrophilic surface. Ohishi and Tanaka reported the formation of porous TiO_2 on the surface of a Ti sheet by immersing the Ti sheet in NaOH solution [16,17]. Tanaka indicated that the presence of TiH_2, formed during the pretreatment, is one of the factors crucial to obtaining a porous TiO_2 membrane on Ti [17]. He explained the reaction mechanism by using the following equation:

$$TiH_2 + 2H_2O \rightarrow TiO_2 + 6H^+ + 6e^- \quad (1)$$

The formation of the porous structure is due to the ability of Ti to absorb hydrogen:

$$H_{ab} + H_2O + e^- \rightarrow H_2 \uparrow + OH^- \quad (2)$$

where H_{ab} is the hydrogen absorbed by Ti. The formed H_2 escapes and leaves holes on the surface, generating its porous structure. Conversely, Ohishi believed that the reaction is driven by the following equation:

$$Ti + 4OH^- \rightarrow TiO_2 + 2H_2O + 4e^- \quad (3)$$

$$Ti + 2H_2O \rightarrow TiO_2 + 2H_2 \quad (4)$$

Although the mechanism of the formation of the porous TiO_2 through the chemical etching of titanium is ambiguous, the influence factor and rules of the reaction process and products are specific. Tanaka reported that pore size and film thickness are significantly influenced by the reaction time, temperature, and concentration of NaOH solution [17,18]. He used 5 M NaOH solution to form the porous TiO_2 membrane and indicated that the products were only Ti and TiO_2 when the solution temperature was 80 °C [18]. Chen obtained a porous TiO_2 membrane using NaOH solutions with relatively low concentrations (0.5 M–4 M). They reported that some titanates formed after a long reaction time at 80 °C, but the main products were TiO_2 [19]. Kamarozaman reported that the final structure of the TiO_2 surface is affected by the position of the substrates in the NaOH solution [20].

Compared with the reported methods for TiO_2 pH sensing films, chemical etching is a simple, safe, mild, and inexpensive one. A porous surface is helpful for enhancing the wettability of an electrode. Thus, it is a promising method for the fabrication of a super-hydrophilic TiO_2 thin film for pH detection.

In this current work, 30 groups of porous TiO_2 films were obtained using the chemical etching method. The polished Ti sheets were immersed in NaOH solution, with solution concentrations of 0.5, 1, 2, 3 and 4 M and reaction times of 15, 30, 60, 120, 180 and 240 min. To determine the optimum fabrication parameters, the obtained electrodes were compared for their wettability and pH sensing performances, including the sensitivity, response time, drift, hysteresis, selectivity, and stability.

2. Materials and Methods

2.1. Fabrication of a Sensitive Electrode with Super-Hydrophilic TiO_2 Thin Film

The degreasing agent was prepared with 50 g/L NaOH, 25 g/L Na_2CO_3, 30 g/L Na_3PO_4, and 2 g/L Triton X-100. A Ti sheet (99.8% purity, 100 × 100 × 0.1 mm, Jinxin Advanced Metal Co., Xingtai, China) was cut to a size of 10 × 30 mm, ultrasonically cleaned in degreasing agent for 20 min, rinsed using deionized water (DI water), and air dried. Subsequently, the Ti sheet was mechanically polished on 1500 mesh abrasive paper and

further polished with aluminum oxide abrasives to a size of 1 μm. The specimen was finally polished with aluminum oxide abrasives to a size of 0.3 μm. Then, it was ultrasonically cleaned with degreasing agent for 10 min and washed with DI water.

Figure 1a shows the fabrication procedure of the super-hydrophilic TiO_2 thin film. The polished Ti sheet was immersed in HF (0.5 wt%, Haibiao, China) for about 100 s to form the white surface. Afterwards, it was washed with DI water and air dried. Then, 0.5, 1, 2, 3 and 4 M NaOH solutions were prepared in 200 mL beakers and placed in a water bath kettle at 80 °C. The Ti sheets were inserted in PTFE baskets to maintain their vertical positioning and immersed in NaOH solutions for 15, 30, 60, 120, 180 or 240 min. Subsequently, the specimens were rinsed with 0.01 M HCl to remove the remaining NaOH. Finally, the Ti sheets were rinsed with DI water and air dried. Figure 1b shows that the prepared sensitive electrode consisted of Al_2O_3 substrates (96% purity, 15 × 30 × 1 mm, Jiawei Ceramic Tech Co., Zhuhai, China) and a treated Ti sheet attached to the substrate.

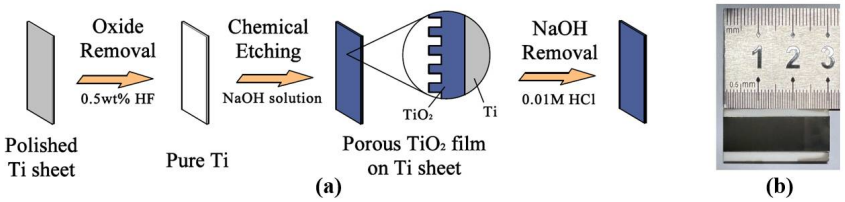

Figure 1. (**a**) Scheme of the sensitive electrode fabrication procedure and (**b**) photograph of the sensitive electrode.

2.2. Characterization of the Porous TiO_2 Films and Their pH Sensing Performance

The morphological and structural characterization of the porous films were investigated by field emission scanning electron microscopy (JSM-7001F, JOEF, Japan), X-ray photoelectron spectroscopy (ESCALAB 250Xi, Thermo Scientific, USA), and X-ray diffractometer (D8 ADVANCE, Bruker, Germany). Wettability was measured using a contact angle meter (JC2000D, POWEREACH, Shanghai, China).

The sensitivity, response time, drift, hysteresis, repeatability, stability, and selectivity of the fabricated electrodes versus a commercial Ag/AgCl reference electrode (E218, Leici, China) were studied to investigate the influence of the chemical etching parameters on the pH sensing performance. The response potential was measured using an electrochemical workstation (CHI660E, Chenhua Instrument, Shanghai, China) and recorded with a computer. pH buffer solutions (PBSs) were prepared by mixing 0.01 M HCl (Beyotime Biotechnology, Shanghai, China) and 0.01 M NaOH solutions with different ratios. pH of each PBS was measured by a commercial glass pH meter (PHS-3E, Leici, China), which was calibrated using standard pH buffer solutions (pH 4.01 and 9.18, Leici, China).

To measure the sensitivity, response time, and potential deviation, each TiO_2 electrode was dipped in the same PBS for 100 s, tested 3 times, cleaned with deionized water, and air dried. The response potentials were recorded at 0.1 s intervals. The drift effect was measured by dipping the electrodes in PBS (pH = 6.86) at 25 °C for 2 h, and the potential was recorded at 2 s intervals. The TiO_2-sensitive electrodes were dipped in PBS with loops of 7.84–5.91–4.41–5.91–7.84–10.13–12.01–10.13–7.84 and 7.84–10.13–12.01–10.13–7.84–5.91–4.41–5.91–7.84 without cleaning and drying to measure the hysteresis width. The TiO_2-sensitive electrode was dipped in each PBS for 200 s, and the potential was recorded at 1 s intervals. To evaluate the selectivity of the developed electrode, 200 μL of 0.1 M KCl, NaCl, $NiCl_2$, $CaCl_2$, and $FeCl_3$ were added to 19.8 mL of prepared PBS to ensure the concentration of interfering ions reached 0.001 M. Each electrode was dipped in the solution for 100 s and tested 3 times.

3. Results and Discussion

3.1. XRD and XPS

XRD and XPS analyses were conducted on electrodes obtained using 1 M–120 min, 1 M–240 min, 4 M–120 min, and 4 M–240 min to investigate the influence of the fabrication parameters. As shown in Figure 2a, titanium and anatase peaks were detected on the pattern of the electrodes treated using different fabrication parameters. The pattern also revealed irregular background noise and no other characteristic peaks, indicating the presence of amorphous TiO_2 film.

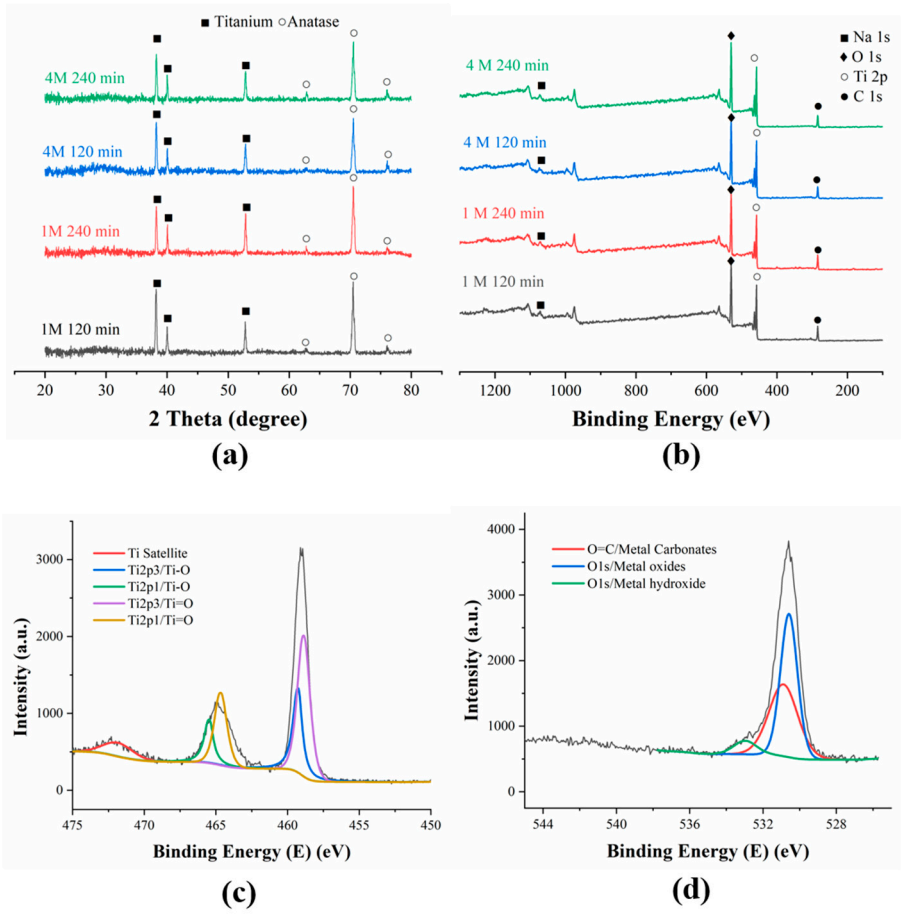

Figure 2. (**a**) XRD and (**b**) XPS pattern of the sensitive electrodes obtained using four typical fabrication parameters, (**c**) Ti 2p, and (**d**) O 1s deconvoluted core excitations for the electrode obtained using 1 M–120 min.

Surface analysis of the films was carried out using XPS and is plotted in Figure 2b. Na 1s, O 1s, Ti 2p, and C 1s peaks were observed in the pattern. The Ti 2p and O 1s deconvoluted core excitations of the electrode treated using 1 M–120 min are presented in Figure 2c,d, respectively, and the core excitations and atomic percentage are listed in Table S1. The Ti 2p and O 1s deconvoluted core excitations of the other three electrodes are plotted in Figure S1. Figure 2c shows that the Ti 2p spectrum exhibits five contributions: Ti-O 2p 3/2, Ti=O 2p 3/2, Ti-O 2p 1/2, Ti=O 2p 1/2, and a satellite state. All Ti 2p spectra from the different electrodes showed a similar envelope. These intensive peaks matched the standard TiO_2 pattern, indicating the main components of the Ti 2p spectrum were assigned to Ti=O and Ti-O in TiO_2. The quantitative analysis confirmed that the main component of all the films obtained with different fabrication parameters was TiO_2. As shown in Figure 2d, the O 1s core excitation was deconvoluted into three components. The most intensive peak was observed at BE. 530.6 eV and assigned to oxygen–metal bonding, which is present in a metal oxides lattice [21]. The component at BE. 533 eV was ascribed

to metal hydroxyl and the component at BE. 530.45 eV was ascribed to a carbon–oxygen double bond, indicating the presence of a small quantity of NaOH and adsorbed CO_2 on the surface.

Tanaka reported weak peaks of rutile and anatase in a film fabricated using GIXRD, indicating their minor production on the surface [17]. Ohishi identified the porous film as TiO_2 using XPS [16]. As shown in Table S1, when the reaction time increased from 120 to 240 min, the atomic percentage of Na increased from 1.92% to 2.28% (1 M NaOH) and 1.49% to 2.61% (4 M NaOH). This result confirmed that the prolonged reaction time led to an increase in the titanate content.

3.2. Morphology

To investigate the influence of the fabrication parameters, SEM was performed on 4 pieces of the electrodes treated with 1 M NaOH and four pieces treated with 4 M NaOH. The reaction time was 15, 60, 120, or 240 min. The original SEM images are presented in Figures 3 and 4, and the SEM images with the size of the pores and ridges are shown in Figures S2 and S3.

As shown in Figure 3a, abundant TiO_2 nanowires and some small holes formed on the surface, and the original surface could still be identified. As estimated from Figures 3a and S2a, the hole diameters were 36.46–66.92 nm, and the ridge thickness was 22.71–36.35 nm. Figure 3b shows that the surface was entirely covered by the TiO_2 nanowires, which combined with one another and formed nets. Meanwhile, more holes were observed on the surface. As shown in Figures 3c and S2c, the ridges ranged from 27.26–39.19 nm, and the diameters ranged from 47.71–60.31 nm, indicating that the microstructures became more uniform and denser than those shown in Figure S2a,b. As shown in Figure 3d, with the further prolonged reaction time, the ridge thickness and hole diameters were enlarged. Tanaka indicated that hydrogen penetration continuously occurs during a reaction, providing sufficient hydrogen to produce porous TiO_2 [18]. Thus, the surface morphology was continuously changed with the prolonged reaction time.

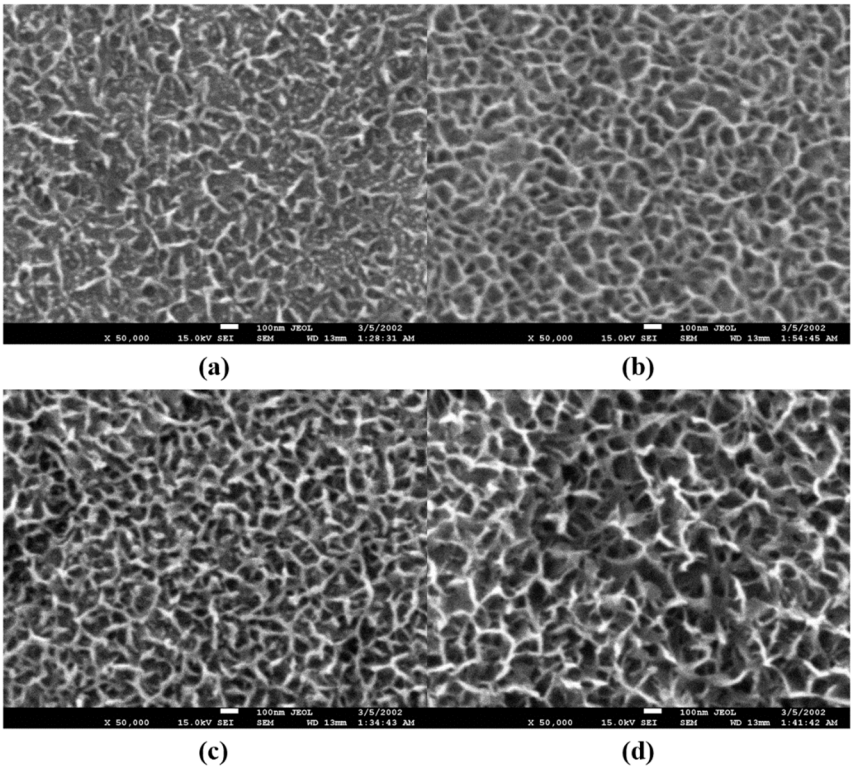

Figure 3. SEM images of TiO_2 electrodes prepared in 1 M NaOH for (**a**) 15, (**b**) 60, (**c**) 120, and (**d**) 240 min.

Figures 4 and S3 show that the original surface can hardly be identified. The holes and ridges are larger than those shown in Figure S2. As estimated from Figure S3a–d, with the prolonged reaction time, the maximum size of the diameters and ridges increased from 75.34 to 134.06 nm and 46.29 to 65.07 nm, respectively, indicating that the higher concentration resulted in a more drastic reaction and a larger-sized microstructures. Tanaka suggested that the hydrogen content increases with an increase in the NaOH concentration as hydrogen penetration is affected by the content of alkali cations in the solution [18,22].

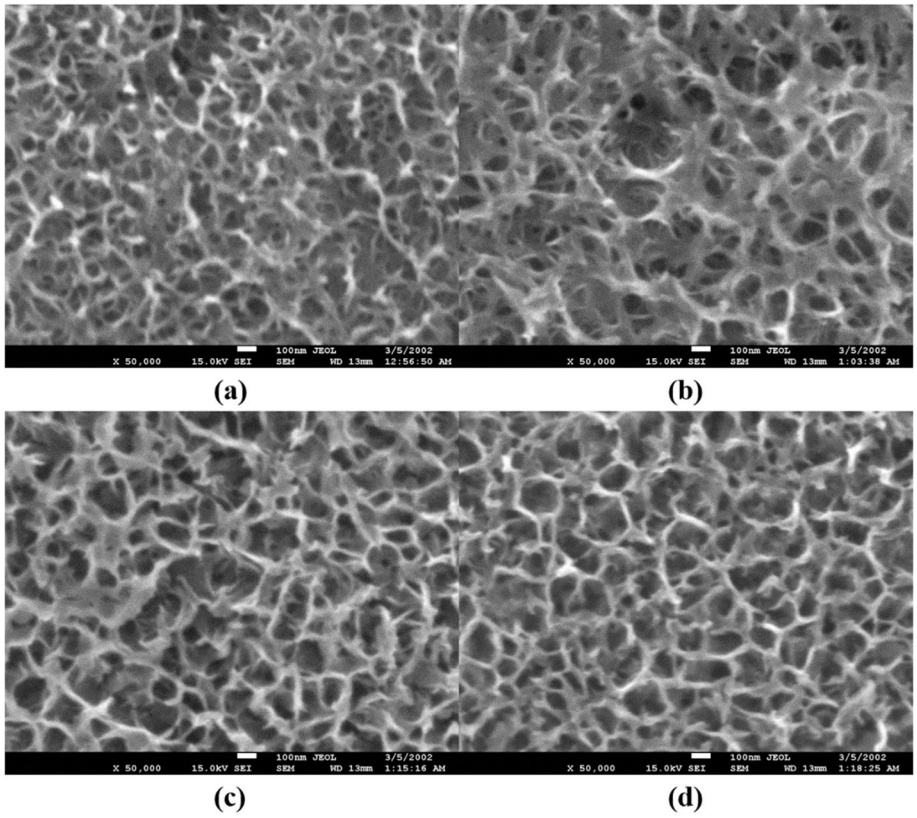

Figure 4. SEM images of TiO_2 electrodes prepared in 4 M NaOH for (**a**) 15, (**b**) 60, (**c**) 120, and (**d**) 240 min.

3.3. Wettability

A super-hydrophilic surface is a material whose water contact angles (CAs) are less than 10° [23]. Figure S4 presents the photographs of the CAs of the electrodes obtained using different fabrication parameters. Figure 5 illustrates the change trend of the CAs. Few electrodes fabricated in 0.5 and 4 M NaOH could satisfy the super-hydrophilic standard, whereas most electrodes obtained in 1, 2, and 3 M NaOH achieved good wettability. Figure 5 also indicates that a short reaction time may result in weak wettability, which could be explained by Wenzel's equation:

$$\cos\theta_e^r = r * \cos\theta_e \quad (5)$$

where ${\theta_e}^r$ represents the apparent contact angle over a practical surface, θ_e is the contact angle on an ideal smooth surface, and r is the roughness of the solid surface, which is described by the specific surface area (SSA). For a hydrophilic surface, an increased r reduces ${\theta_e}^r$ and contributes to a super-hydrophilic case [24–26]. The SEM images showed that increasing the concentration and reaction time enhanced the surface roughness, resulting in increased SSA. Meanwhile, with further continued etching, the wettability of the electrodes was reduced. XPS analysis revealed that the titanate content increased with the prolonged reaction time. Tanaka indicated that porous TiO_2 films have a "sandwich" structure, i.e.,

the titanate covers TiO_2, which forms on the Ti sheet and thus explains the decreased wettability with further prolonged reaction times [17].

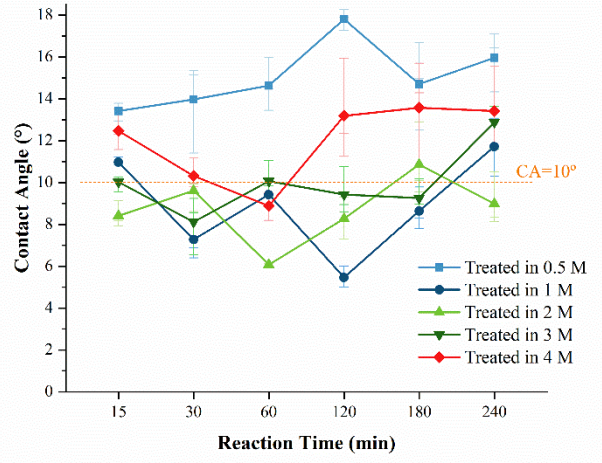

Figure 5. The influence of the fabrication parameters on CA of the electrodes; CA < 10° is described as super-hydrophilic.

3.4. pH Response of the Fabricated Electrodes

3.4.1. Sensitivity

Table S2 indicates that most of the electrodes satisfied the quasi-Nernstian response [27], and the highest sensitivity was 54.13 mV/pH with a correlation coefficient of 0.997. Figure 6 presents the influence of the fabrication parameters on the sensitivity, which apparently depends on the NaOH concentration. The electrodes obtained in 0.5 M and 4 M NaOH showed poor sensitivity, whereas those obtained in 1 M and 2 M NaOH showed high sensitivity.

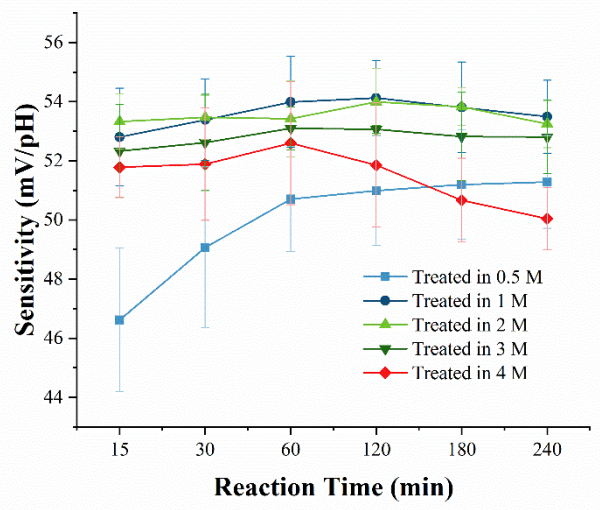

Figure 6. The influences of the fabrication parameters on the sensitivity of the porous TiO_2 electrodes.

As shown in Figure 7, the site-binding theory is used to explain the reaction on the surface of the metal oxides: during the reaction, the surface of the TiO_2-sensitive electrode is covered by hydroxide groups due to the dissociative adsorption of water [28,29], and protons and hydroxide ions from the solution are attracted to oxygen ions from the TiO_2 crystal lattice and to the surface cations, respectively [30–32]. According to the site-bonding model, the sensitivity of the sensing film can be described as [30]:

$$\beta = \frac{2q^2 N_S \sqrt{k_b/k_a}}{kTC_{DL}} \quad (6)$$

where β is the sensitivity of the sensing film, q is the electronic charge, Ns is the total number of sites per unit area, k_a and k_b are equilibrium constants, k is Boltzmann's constant, T is the temperature of the system, and C_{DL} is the double-layer capacitance at the interface. The dense and rough microstructures on the surface lead to an increase in the total number of sites per unit area (Ns) [10]. The sensitivity of the electrodes obtained in 0.5 M NaOH was positively correlated with the reaction time because the surface morphology depends primarily on the reaction time at a low NaOH concentration [18]. The electrodes obtained in 4 M NaOH were negatively correlated with the reaction time, which can be attributed to the increased titanate that formed on TiO_2.

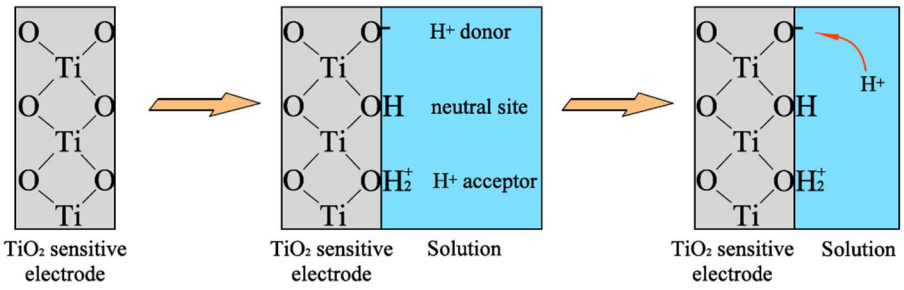

Figure 7. Schematic of the detection principle and procedure of the TiO_2 pH-sensitive electrode.

Compared with other literature, the electrodes obtained in our work did not achieve the highest sensitivity. Zhao reported a pH sensor based on a TiO_2 nanotube array-modified Ti electrode with a sensitivity of 57.1 mV/pH [5]. Liao prepared a pH sensing layer using sol-gel spin coating technology and showed a high pH sensitivity of approximately 58.73 mV/pH [32]. The differences in the sensitivity may contribute to the different fabrication methods and compositions, which affects the microstructure, porosity, surface homogeneity, and crystalline structure [7]. Meanwhile, a small amount of titanates form on, and cover the surface of the sensing film, thereby reducing the hydrophilic sites for H^+ and leading to decreased sensitivity [10].

3.4.2. Response Time

The response time of each electrode is shown in Figure 8. As shown in Figure 8a–e, the response time of each electrode obviously depends on the pH level. The electrodes exhibited a fast response in acidic and neutral solutions but a much slower response in basic ones because of the dominant diffusion of H^+ ions in acidic solutions as reported in the literature [33–36]. As shown in Figure 8f, the response time of the electrodes was obviously affected by the fabrication parameters. Electrodes obtained in the 1, 2, and 3 M NaOH solutions showed a faster response than those obtained in the 0.5 and 4 M solutions. The response time of the electrodes was affected by the structural properties and morphology, indicating that the sensing film with a developed pore network had a fast response time [34,37]. SEM analysis revealed that the pH-sensitive electrodes treated with 1 M NaOH showed more uniform and denser microstructures on the surface than those treated with 4 M NaOH, so the former exhibited a faster response.

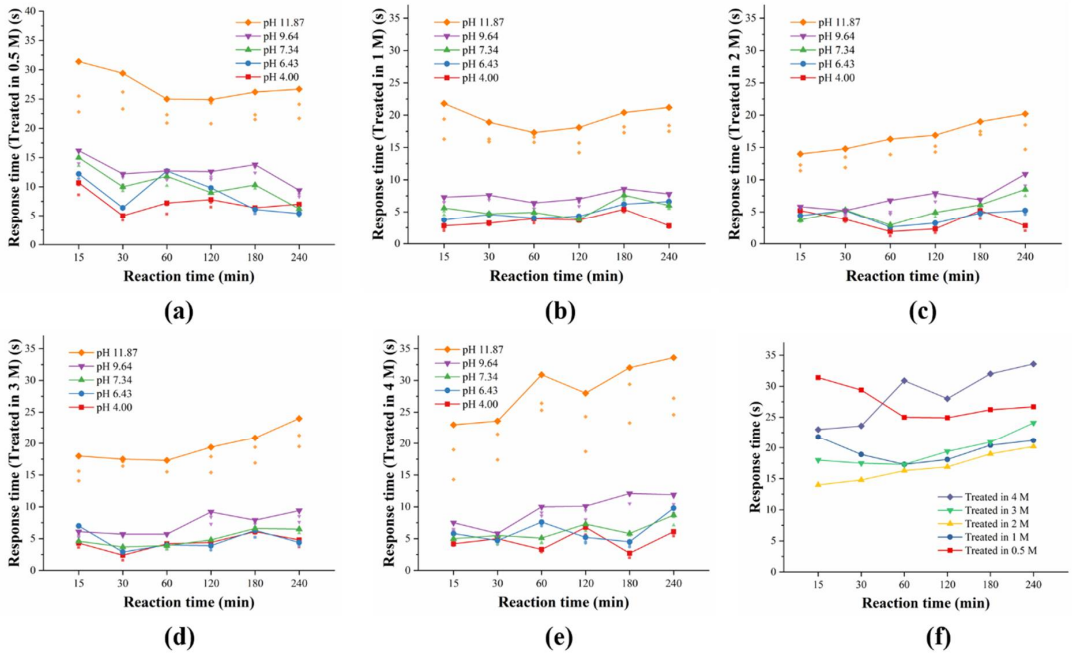

Figure 8. The influences of the fabrication parameters and pH levels on the response time of the sensitive electrodes treated in (**a**) 0.5 M, (**b**) 1 M, (**c**) 2 M, (**d**) 3 M, (**e**) 4 M and (**f**) the response time of each electrode.

3.4.3. Potential Deviation

Potential deviation is defined herein to enable an investigation of the electrodes' short-term stability. It is described as the potential difference between the peak potential value and the potential at a response time within 60 s. Each electrode was tested three times and the average potential deviations are presented in Figures 9a and 8e (note the ordinate value of Figure 9a). Figure 9f shows the maximum potential deviation of each electrode at different pH levels.

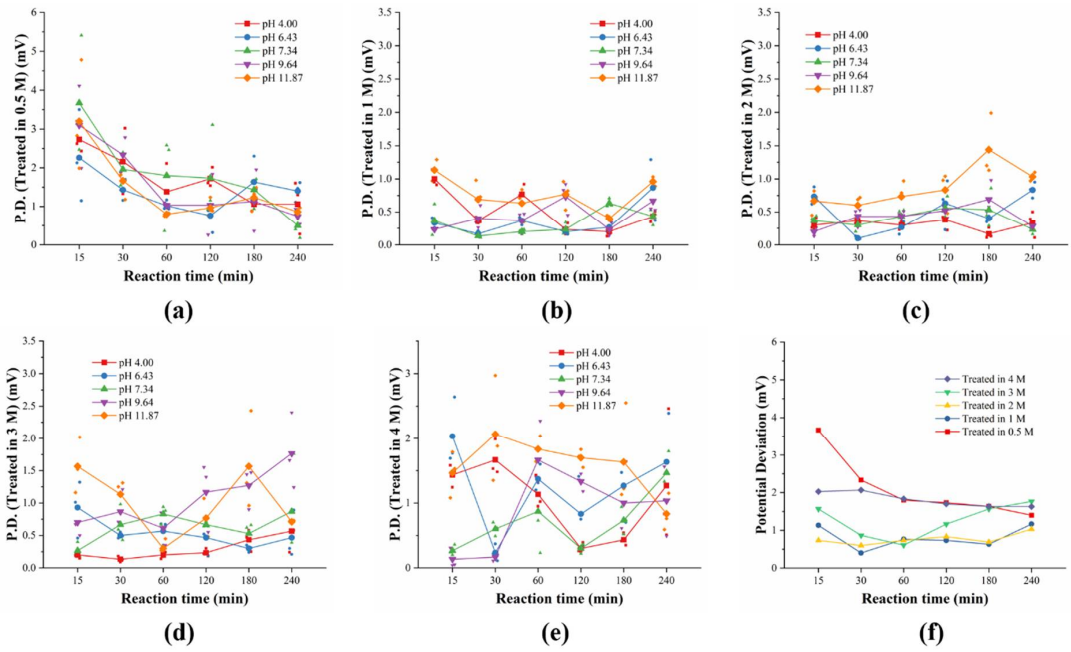

Figure 9. The influences of the fabrication parameters and pH levels on the potential deviation (P.D.) of the sensitive electrodes treated in (**a**) 0.5 M, (**b**) 1 M, (**c**) 2 M, (**d**) 3 M, (**e**) 4 M and (**f**) the potential deviation of each electrode.

Figure 9a–e show that the potential deviation of the electrode also depended on the fabrication parameters but not the pH levels. Figure 9f indicates that electrodes obtained in 1 and 2 M NaOH solutions showed relatively low potential deviations, ranging from 0.63 to 1.17 mV. Thus, the drift effect of the electrodes treated with 1 and 2 M NaOH solutions was further studied.

3.4.4. Drift Effect

The drift effect was explored using 4 pieces of electrodes treated with 1 M NaOH and 4 pieces treated with 4 M NaOH for various reaction times (15, 60, 120, or 240 min). As listed in Table 1, with an increase in the reaction time from 15 to 240 min, the drift of the electrodes obtained in 1 and 2 M NaOH solutions showed an apparent decrease from 36.18 to 6.4 mV/h and 22.53 to 5.16 mV/h, respectively. Similarly, the increased solution concentration also resulted in decreased drift.

Compared with previous results, the drift of the prepared electrode was relatively high, which may contribute to the high resistance and intrinsic properties of TiO_2 films [37]. Yusof reported a TiO_2 sensing membrane fabricated using the RF sputtering method with a drift of 4.41 mV/h. Chou doped ruthenium metallic ions on TiO_2 film using a co-sputtering system to decrease the resistivity and increase its carrier mobility, which resulted in a very low drift effect of 1.67 mV/h [38].

Table 1. Drift of the electrodes treated using different fabrication parameters.

Solution Concentration	Reaction Time (min)			
	15	**60**	**120**	**240**
1 M	36.18 mV/h	15.27 mV/h	9.29 mV/h	6.4 mV/h
2 M	22.53 mV/h	9.38 mV/h	7.11 mV/h	5.16 mV/h

3.4.5. Hysteresis

The hysteresis widths of the electrodes are listed in Table 2. The results showed that the increased NaOH concentration and reaction time decreased the hysteresis width. The hysteresis width of the TiO_2 pH sensor was reported to be 30 mV in the cycle of 2–12–2 by Fog and Buck in 1984 [39]. Afterwards, few studies have mentioned the hysteresis width of TiO_2-based pH electrodes. Compared with other metal oxide-based pH-sensitive electrodes, the prepared electrodes showed a relatively high hysteresis. Xu reported an RuO_2 pH sensor fabricated using the magnetron sputtering method with a hysteresis of 6.4 mV in the loop of 7–4–7–10–7 and 5.1 mV in the loop of 7–10–7–4–7 [40]. An electrodeposited iridium oxide pH sensor was reported to have a hysteresis of 0.5–1.5 in neutral solution. Santos used the hydrothermal synthesis method to develop a WO_3 pH sensor with a hysteresis of 6–10 mV [41]. This feature may contribute to the intrinsic properties, the surface area, crystalline properties, and the composition of TiO_2 films [7].

Table 2. Hysteresis width of the tested electrodes.

Fabrication Parameters	Hysteresis in Loop 1	Hysteresis in Loop 2
1 M 60 min	17.6 mV	19.3 mV
1 M 120 min	8.9 mV	11.4 mV
2 M 60 min	10 mV	10.5 mV
2 M 120 min	7.3 mV	9.5 mV

3.4.6. Repeatability

Based on the characterization studies, 1 M and 120 min were selected as the optimum fabrication parameters for the super-hydrophilic TiO_2 pH electrode. The SEM image confirmed the presence of dense and uniform microstructures on the surface, leading to its small CA of 5.46°. It also showed the highest sensitivity of 54.13 mV/pH, a fast response of 18.1 s in pH 4–12, an acceptable drift of 9.29 mV/h, and a hysteresis width of 11.4 mV.

Subsequently, a new series of electrodes were fabricated to evaluate their repeatability. Thus, 2 electrodes from the initial lot (electrodes A1 and A2) and 2 from the new lot (electrodes B1 and B2) were dipped in PBS with different pH levels for 300 s, respectively. The OCP changes were recorded at 1 s intervals, and the results are presented in Figure 10. The electrodes from the different lots showed stable and consistent response potentials for each pH level. As shown in Table 3, the electrodes from the new lot showed a similar Nernstian response, with a sensitivity of 53.47 and 54.58 mV/pH. Thus, the discrepancy in the sensitivity for the different lots was less than 1.95 mV/pH, indicating the good repeatability compared with previously reported electrodes [35].

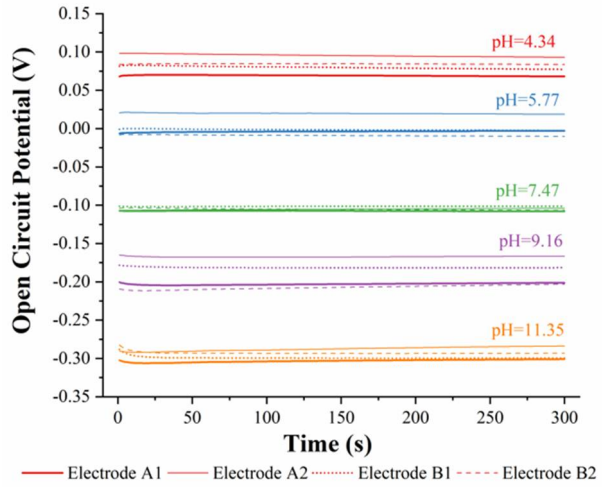

Figure 10. OCP of the electrode obtained from two lots in different pH levels to demonstrate the repeatability.

Table 3. The pH sensing characteristics of the electrodes obtained from different lots.

Sample	Sensitivity	Correlation Coefficient	Response Time
Electrode A1	52.63	0.996	16 s
Electrode A2	53.79	0.989	18 s
Electrode B1	53.47	0.998	20 s
Electrode B2	54.58	0.987	17 s

3.4.7. Selectivity

The selectivity coefficient of an electrode characterizes its ability to distinguish a particular ion from others and is commonly evaluated using the fixed interference method (FIM), which is defined by the following equation:

$$K_{ij}^{pot} = \exp\left(\frac{Z_i F}{RT}\left(E_j^0 - E_i^0\right)\right) \quad (7)$$

where F is Faraday Constant, R is gas constant, T is Kelvin Temperature, E is the experimentally measured potential, E_i^0 is a constant that includes the standard sensing potential of the primary ion, E_j^0 is the sensing potential of the interfering ion, and Z_i is the charge numbers of the principal ion I [33].

The interference effects of the five cations are compared in Table 4. The selectivity coefficients of the fabricated electrodes for Na^+, K^+, Ca^{2+}, Ni^{2+}, and Fe^{3+} were −3.02, −3.44, −2.51, −3.52, and −3.29, respectively. The selectivity coefficients for the tested interfering ions were smaller than 1 and K_{ij}^{pot} was less than 10^{-2}, indicating its good selectivity [42,43].

Table 4. The selectivity coefficients of the fabricated electrode for Na^+, K^+, Ca^{2+}, Ni^{2+}, and Fe^{3+}.

Primary Cation	Interfering Cation	Concentration of Interfering Cation	K_{ij}^{pot}	Log (K_{ij}^{pot})
H^+	Na^+	0.001 M	9.54×10^{-4}	−3.02
	K^+		3.61×10^{-4}	–3.44
	Ca^{2+}		3.14×10^{-3}	–2.51
	Ni^{2+}		2.97×10^{-4}	–3.52
	Fe^{3+}		5.11×10^{-4}	–3.29

3.4.8. Stability of the Super-Hydrophilic TiO_2-Sensitive Electrode

The fabricated electrodes were stored in a clean and dry box, which was placed in the dark and was not hermetic. As listed in Table S3, after storage for 60 days, CA of the 2 electrodes changed from 5.93° to 7.43° and 6.37° to 7.48°, respectively. The sensitivity of the electrodes changed from 52.71 and 52.49 mV/pH to 52.74 and 50.83 mV/pH (shown in Figure 11a and Table S3). The small difference in the CA and sensitivity within 60 days indicated the good continuous wettability and pH sensing performance of the electrodes during storage.

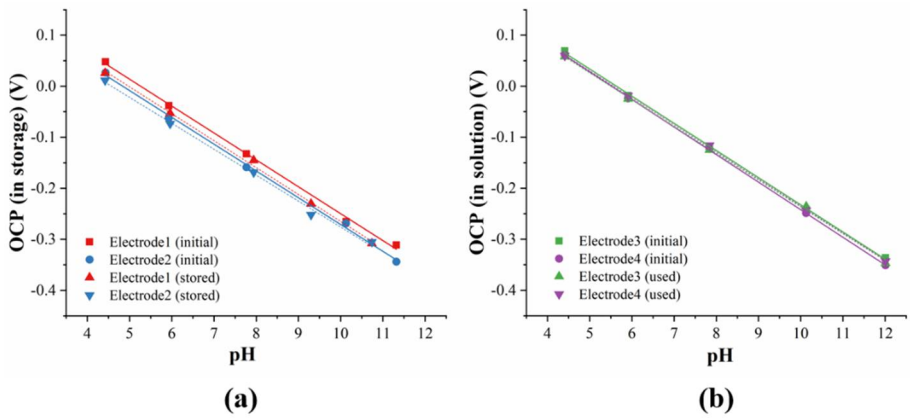

Figure 11. Involution in the sensitivity of the electrodes (**a**) after storage for 60 days and (**b**) when utilized in PBS for 30 min.

The difference in the electrodes before and after pH measurement in the solutions was also investigated. Table S3 shows that the CA of the 2 other electrodes showed small increases of 2.43° and 0.36° after being used for 1800 s and still satisfied the super-hydrophilic surface standard. Figure 11b shows that the electrode sensitivity was almost the same before and after being dipped in solutions with different pH levels.

4. Conclusions

In this work, super-hydrophilic TiO_2 pH-sensitive electrodes were fabricated using the chemical etching method. The influence of the chemical etching parameters (solution concentration and reaction time) on the structure, morphology, wettability, and pH response of the porous films was investigated. With an increased NaOH concentration and reaction time, the surface microstructures became denser and more uniform, improving the wettability, pH sensitivity, and response time of the electrodes. However, a further increase in the NaOH concentration and reaction time led to large and unevenly sized microstructures and an increased presence of titanate, resulting in poor pH wettability, pH sensitivity, and response time, and low drift and hysteresis, indicating the stabler structure of the films.

The electrode obtained using 1 M and 120 min is the optimal product due to its good wettability, with a contact angle of 5.46°, a high sensitivity of 54.13 mV/pH, a response time of 18.1 s in pH 4–12, an acceptable drift of 9.29 mV/h, a hysteresis width of 11.4 mV,

and good selectivity for Na^+, K^+, Ca^{2+}, Ni^{2+}, and Fe^{3+}. The electrode also showed good stability in wettability and pH sensing properties during storage and utilization in PBS.

Supplementary Materials: The following supporting information can be downloaded at: https://www.mdpi.com/article/10.3390/chemosensors10050182/s1, Figure S1: Ti 2p deconvoluted core excitations for electrode treated by using (a)1 M–240 min, (b) 4 M–120 min, (c) 4 M–240 min, and O 1s deconvoluted core excitations for electrode treated by using (d)1 M–240 min, (e) 4 M–120 min, (f) 4 M–240 min. Figure S2: SEM images of TiO_2 electrodes prepared in 1 M NaOH for (a) 15 min, (b) 60 min, (c) 120 min and (d) 240 min with the size of pores and ridges. Figure S3: SEM images of TiO_2 electrodes prepared in 4 M NaOH for (a) 15 min, (b) 60 min, (c) 120 min and (d) 240 min the size of pores and ridges. Figure S4: One μL water droplet contact angle measurements on the electrodes obtained with different fabrication parameters. Table S1: The atomic ratios and parameters of the deconvoluted XPS spectra for different electrodes. Table S2: Sensitivity of the electrodes treated with different fabrication parameters. Table S3. Comparation of the sensitivity and CA of the electrodes before and after utilization/storage.

Author Contributions: Conceptualization, C.C., K.X. and X.Z.; methodology, C.C., Y.Z. and H.G.; validation, C.C., Y.Z. and H.G.; investigation, C.C. and Y.Z.; resources, X.Z.; data curation, C.C.; writing—original draft preparation, C.C.; writing—review and editing, C.C. and K.X.; visualization, C.C.; supervision, X.Z.; project administration, X.Z.; funding acquisition, X.Z. All authors have read and agreed to the published version of the manuscript.

Funding: This research was funded by National Natural Science Foundation of China, grant number 32071900; Jiangsu Postgraduate Research Innovation Program of China, grant number KYCX17_1758.

Institutional Review Board Statement: Not applicable.

Informed Consent Statement: Not applicable.

Data Availability Statement: Not applicable.

Acknowledgments: The authors would like to thank the School of Mechanical Engineering at Jiangsu University for supporting this research and providing the appropriate research environment.

Conflicts of Interest: The authors declare no conflict of interest.

References

1. Wang, R.; Hashimoto, K.; Fujishima, A.; Chikuni, M.; Kojima, E.; Kitamura, A.; Shimohigoshi, M.; Watanabe, T. Light-Induced Amphiphilic Surfaces. *Nature* **1997**, *388*, 431–432. [CrossRef]
2. Farahani, E.; Mohammadpour, R. Fabrication of Flexible Self-Powered Humidity Sensor Based on Super-Hydrophilic Titanium Oxide Nanotube Arrays. *Sci. Rep.* **2020**, *10*, 13032. [CrossRef] [PubMed]
3. Gao, K.; Wang, X.; Yang, B.; Chen, X.; Li, X.; Liu, J. A Novel Wearable Sweat Rate Sensor for Both Dominant and Recessive Sweat Rate Measurement. In Proceedings of the 2019 20th International Conference on Solid-State Sensors, Actuators and Microsystems & Eurosensors XXXIII (Transducers & Eurosensors XXXIII), Berlin, Germany, 23–27 June 2019; IEEE: Berlin/Heidelberg, Germany, 2019; pp. 817–820.
4. Zamarreño, C.R.; Bravo, J.; Goicoechea, J.; Matias, I.R.; Arregui, F.J. Response Time Enhancement of PH Sensing Films by Means of Hydrophilic Nanostructured Coatings. *Sens. Actuators B Chem.* **2007**, *128*, 138–144. [CrossRef]
5. Zhao, R.; Xu, M.; Wang, J.; Chen, G. A PH Sensor Based on the TiO_2 Nanotube Array Modified Ti Electrode. *Electrochim. Acta* **2010**, *55*, 5647–5651. [CrossRef]
6. Zhang, X.; Lu, C.; Geng, M.; Xu, K.; Zong, S. Effects of Surface Area on All-Solid-Stated PH Sensor Based on Antimony Electrode. *IEEE Sens. J.* **2020**, *20*, 680–688. [CrossRef]
7. Manjakkal, L.; Szwagierczak, D.; Dahiya, R. Metal Oxides Based Electrochemical PH Sensors: Current Progress and Future Perspectives. *Prog. Mater. Sci.* **2020**, *109*, 100635. [CrossRef]
8. Yao, P.C.; Lee, M.C.; Chiang, J.L. Annealing Effect of Sol-Gel TiO_2 Thin Film on PH-EGFET Sensor. In Proceedings of the 2014 International Symposium on Computer, Consumer and Control, Taichung, Taiwan, 10–12 June 2014; IEEE: Taichung, Taiwan, 2014; pp. 577–580.
9. Yusof, K.A.; Abdul Rahman, R.; Zulkefle, M.A.; Herman, S.H.; Abdullah, W.F.H. EGFET PH Sensor Performance Dependence on Sputtered TiO_2 Sensing Membrane Deposition Temperature. *J. Sens.* **2016**, *2016*, 1–9. [CrossRef]
10. Huang, Y.-C.; Tsai, F.-S.; Wang, S.-J. Preparation of TiO_2 Nanowire Arrays through Hydrothermal Growth Method and Their PH Sensing Characteristics. *Jpn. J. Appl. Phys.* **2014**, *53*, 06JG02. [CrossRef]

11. Doghmane, H.E.; Touam, T.; Chelouche, A.; Challali, F.; Bordji, B. Investigation of the Influences of Post-Thermal Annealing on Physical Properties of TiO_2 Thin Films Deposited by RF Sputtering. *Semiconductors* **2020**, *54*, 268–273. [CrossRef]
12. Sirghi, L.; Hatanaka, Y. Hydrophilicity of amorphous TiO_2 ultra-thin films. *Surf. Sci.* **2003**, *530*, L323–L327. [CrossRef]
13. Sakai, N.; Fujishima, A.; Watanabe, T.; Hashimoto, K. Quantitative Evaluation of the Photoinduced Hydrophilic Conversion Properties of TiO_2 Thin Film Surfaces by the Reciprocal of Contact Angle. *J. Phys. Chem. B* **2003**, *107*, 1028–1035. [CrossRef]
14. Sun, R.-D.; Nakajima, A.; Fujishima, A.; Watanabe, T.; Hashimoto, K. Photoinduced Surface Wettability Conversion of ZnO and TiO_2 Thin Films. *J. Phys. Chem. B* **2001**, *105*, 1984–1990. [CrossRef]
15. Karuppuchamy, S.; Jeong, J.M. Super-Hydrophilic Amorphous Titanium Dioxide Thin Film Deposited by Cathodic Electrodeposition. *Mater. Chem. Phys.* **2005**, *93*, 251–254. [CrossRef]
16. Oishi, T.; Matsubara, T.; Katagirl, A. Formation of Porous TiO_2 by Anodic Oxidation and Chemical Etching of Titanium. *Electrochemistry* **2000**, *68*, 106–111. [CrossRef]
17. Tanaka, S.; Aonuma, M.; Hirose, N.; Tanaki, T. The Preparation of Porous TiO_2 by Immersing Ti in NaOH Solution. *J. Electrochem. Soc.* **2002**, *149*, 167. [CrossRef]
18. Tanaka, S.; Hirose, N.; Tanaki, T. Effect of the Temperature and Concentration of NaOH on the Formation of Porous TiO_2. *J. Electrochem. Soc.* **2005**, *152*, 789. [CrossRef]
19. Chen, J.; Liu, Z.; Zhou, H.; Zheng, Y. A Study on Preparation of TiO_2 Thin Films by Alkali Treatment of Ti Foils. *J. Chem. Eng. Chin. Univ.* **2013**, *6*, 1051–1057. [CrossRef]
20. Kamarozaman, N.S.; Asiah, M.N.; Aznilinda, Z.; Bakar, R.A.; Abdullah, W.F.H.; Herman, S.H.; Rusop, M. Memristive Behavior of TiO_2 Nanostructures Grown at Different Substrate Positioning by Immersion Method. *AMR* **2013**, *795*, 256–259. [CrossRef]
21. Manjakkal, L.; Cvejin, K.; Kulawik, J.; Zaraska, K.; Szwagierczak, D.; Socha, R.P. Fabrication of Thick Film Sensitive RuO_2-TiO_2 and Ag/AgCl/KCl Reference Electrodes and Their Application for PH Measurements. *Sens. Actuators B Chem.* **2014**, *204*, 57–67. [CrossRef]
22. Morozumi, T.; Mizuno, T.; Kurachi, T. Hydrogen Absorption in Cathodically Polarized Zirconium. *Corros. Eng.* **1979**, *28*, 285–291. [CrossRef]
23. Otitoju, T.A.; Ahmad, A.L.; Ooi, B.S. Superhydrophilic (Superwetting) Surfaces: A Review on Fabrication and Application. *J. Ind. Eng. Chem.* **2017**, *47*, 19–40. [CrossRef]
24. Extrand, C.W.; Moon, S.I.; Hall, P.; Schmidt, D. Superwetting of Structured Surfaces. *Langmuir* **2007**, *23*, 8882–8890. [CrossRef] [PubMed]
25. Feng, X.J.; Jiang, L. Design and Creation of Superwetting/Antiwetting Surfaces. *Adv. Mater.* **2006**, *18*, 3063–3078. [CrossRef]
26. Yuan, J.; Liu, X.; Akbulut, O.; Hu, J.; Suib, S.L.; Kong, J.; Stellacci, F. Superwetting Nanowire Membranes for Selective Absorption. *Nat. Nanotech* **2008**, *3*, 332–336. [CrossRef]
27. Yang, S.-Y.; Chen, C.-W.; Chou, J.-C. Investigation on the Sensitivity of TiO_2:Ru PH Sensor by Taguchi Design of Experiment. *Solid-State Electron.* **2012**, *77*, 82–86. [CrossRef]
28. Trasatti, S. Physical Electrochemistry of Ceramic Oxides. *Electrochim. Acta* **1991**, *36*, 225–241. [CrossRef]
29. Mihell, J.A.; Atkinson, J.K. Planar Thick-Film PH Electrodes Based on Ruthenium Dioxide Hydrate. *Sens. Actuators B Chem.* **1998**, *48*, 505–511. [CrossRef]
30. Yates, D.E.; Levine, S.; Healy, T.W. Site-Binding Model of the Electrical Double Layer at the Oxide/Water Interface. *J. Chem. Soc. Faraday Trans. 1* **1974**, *70*, 1807. [CrossRef]
31. Al-Hilli, S.; Willander, M. The PH Response and Sensing Mechanism of N-Type ZnO/Electrolyte Interfaces. *Sensors* **2009**, *9*, 7445–7480. [CrossRef]
32. Liao, Y.-H.; Chou, J.-C. Preparation and Characterization of the Titanium Dioxide Thin Films Used for PH Electrode and Procaine Drug Sensor by Sol–Gel Method. *Mater. Chem. Phys.* **2009**, *114*, 542–548. [CrossRef]
33. Huang, W.-D.; Cao, H.; Deb, S.; Chiao, M.; Chiao, J.C. A Flexible PH Sensor Based on the Iridium Oxide Sensing Film. *Sens. Actuators A Phys.* **2011**, *169*, 1–11. [CrossRef]
34. Manjakkal, L.; Zaraska, K.; Cvejin, K.; Kulawik, J.; Szwagierczak, D. Potentiometric RuO_2–Ta2O5 PH Sensors Fabricated Using Thick Film and LTCC Technologies. *Talanta* **2016**, *147*, 233–240. [CrossRef] [PubMed]
35. Manjakkal, L.; Cvejin, K.; Kulawik, J.; Zaraska, K.; Szwagierczak, D.; Stojanovic, G. Sensing Mechanism of RuO_2–SnO_2 Thick Film PH Sensors Studied by Potentiometric Method and Electrochemical Impedance Spectroscopy. *J. Electroanal. Chem.* **2015**, *759*, 82–90. [CrossRef]
36. Telli, L. Study of a PH Sensor with MnO_2 and Montmorillonite-Based Solid-State Internal Reference. *Solid State Ion.* **2000**, *128*, 255–259. [CrossRef]
37. Zhuiykov, S.; Kats, E.; Kalantar-zadeh, K.; Breedon, M.; Miura, N. Influence of Thickness of Sub-Micron Cu2O-Doped RuO_2 Electrode on Sensing Performance of Planar Electrochemical PH Sensors. *Mater. Lett.* **2012**, *75*, 165–168. [CrossRef]
38. Jung-Chuan Chou; Cheng-Wei Chen Fabrication and Application of Ruthenium-Doped Titanium Dioxide Films as Electrode Material for Ion-Sensitive Extended-Gate FETs. *IEEE Sens. J.* **2009**, *9*, 277–284. [CrossRef]
39. Fog, A.; Buck, R.P. Electronic Semiconducting Oxides as PH Sensors. *Sens. Actuators* **1984**, *5*, 137–146. [CrossRef]
40. Xu, B.; Zhang, W.-D. Modification of Vertically Aligned Carbon Nanotubes with RuO_2 for a Solid-State PH Sensor. *Electrochim. Acta* **2010**, *55*, 2859–2864. [CrossRef]

41. Santos, L.; Neto, J.P.; Crespo, A.; Nunes, D.; Costa, N.; Fonseca, I.M.; Barquinha, P.; Pereira, L.; Silva, J.; Martins, R.; et al. WO_3 Nanoparticle-Based Conformable PH Sensor. *ACS Appl. Mater. Interfaces* **2014**, *6*, 12226–12234. [CrossRef]
42. Umezawa, Y.; Bühlmann, P.; Umezawa, K.; Tohda, K.; Amemiya, S. Potentiometric Selectivity Coefficients of Ion-Selective Electrodes. Part I. Inorganic Cations (Technical Report). *Pure Appl. Chem.* **2000**, *72*, 1851–2082. [CrossRef]
43. Maleki, R.; Matin, A.A.; Jouyban, A. A Membrane Sensor for Selective Determination of Bisacodyl in Tablets. *J. Chin. Chem. Soc.* **2006**, *53*, 613–618. [CrossRef]